

The new 2018 version of Meudon spectroheliograph

J.-M. Malherbe¹ · K. Dalmasse²

© Springer ●●●

Abstract Daily **full-disk** observations of the solar photosphere and chromosphere started at Meudon Observatory in 1908. After a review of the scientific context and the historical background, we describe the instrumental characteristics and capabilities of the new version operating since 2018. The major change is the systematic recording of full line profiles over the entire solar disk providing 3D data cubes. Spectral and spatial sampling are both improved. Classical 2D images of the Sun at fixed wavelength are still delivered. We summarize the different processing levels of on-line data and briefly review the new scientific perspectives.

Keywords: photosphere; chromosphere; spectroheliograph; full-sun; long-term observations

1. Introduction

Systematic observations of the solar disk started at Meudon Observatory in 1908 with Deslandres's spectroheliograph. The collection is one of the largest available to the international community with 10 observed cycles (observations were just interrupted during the first world war). It contains mainly monochromatic images in wavelengths as H α (center), CaII K1v (violet wing) and CaII K3 (center). A few spectroheliographs were built at about the same time at Mount Wilson (USA, Hale, 1907; Bertello, Ulrich, and Boyden, 2010), Kodaikanal (India, Hasan *et al.*, 2010) and Coimbra (Portugal, Garcia *et al.*, 2011). Meudon and Coimbra spectroheliographs are still in activity.

Most present full-disk observations of the Sun are performed with narrow band imagers as Fabry P erot filters (e.g. GONG H α network, Harvey *et al.*, 2011) or Lyot filters (e.g. GHN H α network, Gallagher *et al.*, 2002). Spectroheliographs, however, operate in spectroscopic mode and the 2018 release provides 3D data cubes (x, y, λ), λ being the wavelength along line profiles and (x, y) the spatial coordinates on the Sun.

¹ LESIA, Observatoire de Paris, 92195 Meudon, and PSL Research University, France, email: Jean-Marie.Malherbe@obspm.fr

² IRAP, Universit e de Toulouse, CNRS, CNES, UPS, 31028 Toulouse, France, email: Kevin.Dalmasse@irap.opm.eu

This work is for the purpose of promoting the studies requiring **full-disk spectral data and/or long-term observations**. Section 2 recalls the scientific **interest of long-term archives in solar physics**. In section 3, we present an historical background summarizing evolutions of Meudon spectroheliograph from the end of the 19th century up to now. Section 4 describes the instrumental characteristics and capabilities of the 2018 version. **The data taken with the new spectrograph are widely open to the community as explained in Section 5**. Finally, section 6 discusses new perspectives.

2. Scientific context of spectroheliograms and long-term observations

The 110-year-old Meudon collection contains **full-disk** spectroheliograms that are relevant to research on the solar cycle, activity, and space weather. CaII K1v data allow to analyze photospheric properties of active regions (ARs), while H α reveals solar filaments. Such data are used to produce synoptic maps of sunspots, faculae and filaments (Martres and Zlicaric 1982, and monthly publications by D’Azambuja 1920 in *l’Astronomie* during the 1928-2003 period). This in turn provides information on the evolution of solar structures during the cycle, including the equatorward migration of ARs (Makarov and Sivaraman, 1989; Mouradian and Soru-Escout, 1993; Charbonneau, 2010) and the poleward migration of high latitude filaments (Mouradian and Soru-Escout, 1994; Karna, Pesnell, and Zhang, 2015).

Sunspot number and area derived from **full-disk** CaII K1v observations, as well as filament number and length derived from H α , further characterize the amplitude, duration and activity level of the solar cycle (Schwabe, 1844; Wolf, 1861; Hale *et al.*, 1919; Hoyt and Schatten, 1998; Hathaway, Wilson, and Reichmann, 2002; Petrovay, 2010). Quiescent H α filaments delineate large cells of opposite magnetic polarities which allowed Leroy, Bommier, and Sahal-Brechot (1983) to evidence different topologies of prominence magnetic support. When analyzed over long periods, data series help to study the cycle-to-cycle variability (long-term modulations such as the Gleissberg cycle or grand minima as Maunder minimum, see the review by Hathaway, 2010).

Long-term collections of **full-disk** observations provide constraints to improve our understanding of the solar dynamo and its variations (e.g. Tobias, 2002; Norton, Charbonneau, and Passos, 2014). Mein and Ribes (1990) used some structures of spectroheliograms (spots and faculae) as magnetic tracers to evidence large scale motions. Ribes and Bonfond (1990) found the presence of zonal meridional circulation at several latitudes suggesting rolls below the surface.

Full-disk CaII K1v and H α centennial archives are also useful to study extreme solar flares such as the Carrington event (Carrington, 1859; Hodgson, 1859) or the two-ribbon flare of July 25, 1946 (Ellison, 1946). The largest sunspot region ever seen was registered on April 5, 1947, and questioned researchers on the maximum size of groups (Aulanier *et al.*, 2013). Extreme events, in terms of size and energy, are rare. Studying them requires long-term archives which

contribute to develop prediction tools for space weather applications (Schrijver *et al.*, 2012; Schmieder, 2018).

Several works proposed new proxies to extract information from archives. Pevtsov *et al.* (2016) developed a proxy to derive magnetic flux in the plage and sunspots from CaII spectroheliograms. This proxy will be important for pseudo-magnetogram reconstruction from CaII data prior to 1974. It can be used to estimate the amount of magnetic energy available for flares using scaling laws derived from observations (Crosby, Aschwanden, and Dennis, 1993; Shimizu and Tsuneta, 1997; Krucker and Benz, 1998; Parnell and Jupp, 2000) or from MHD models (Aulanier *et al.*, 2013). Toriumi *et al.* (2017) defined a proxy to estimate the flare energy from bright ribbons observed in H α .

Long-term archives can suffer from various artifacts (e.g. over-exposure, aging and defects of support, lack of photometric calibration, missing temporal coverage). This can limit the analysis of the data and the robustness of the results. Chatzistergos *et al.* (2018) recently proposed a new method for automated processing and photometric calibration of CaII spectroheliograms. It allows to consistently combine and process images from different instruments and observatories, in order to build datasets with better temporal coverage. Such a method will be valuable for reconstructions of the solar irradiance (Fontenla *et al.*, 2011; Lean, 2018) for investigating long-term evolution and possible impact on Earth climate (see the review by Haigh, 2007).

In this context, the 2018 release of Meudon spectroheliograph has two major goals:

- **improve the spectroscopic capabilities of the former instrument (better spectral and spatial sampling, better wavelength centering of images)**
- **develop the scientific potential by providing full line profiles over the entire Sun and adding new lines as CaII H (later CaII infra red), allowing thermodynamical diagnostics**

3. Historical background of Meudon spectroheliograph

The fast expansion of spectroscopy began 150 years ago. In 1868, Janssen and Lockyer made the famous discovery of Helium through observation of the He I D3 587.5 nm line in the chromosphere. In 1869, Young discovered the coronium (Fe XIV green line identified 70 years later) in eclipse spectra. These fantastic results (see Secchi, 1875, for the detailed history) initiated the development of solar spectroscopy, leading to the spectroheliograph invention in 1892 by two astronomers in France and USA at the same time (papers by Deslandres, 1909; Hale, 1907).

The basic idea of spectroheliographs is to produce monochromatic images of the solar photosphere and chromosphere using narrow bandpass spectroscopic scans of strong Fraunhofer lines. For that purpose, Meudon spectroheliograph was characterized by:

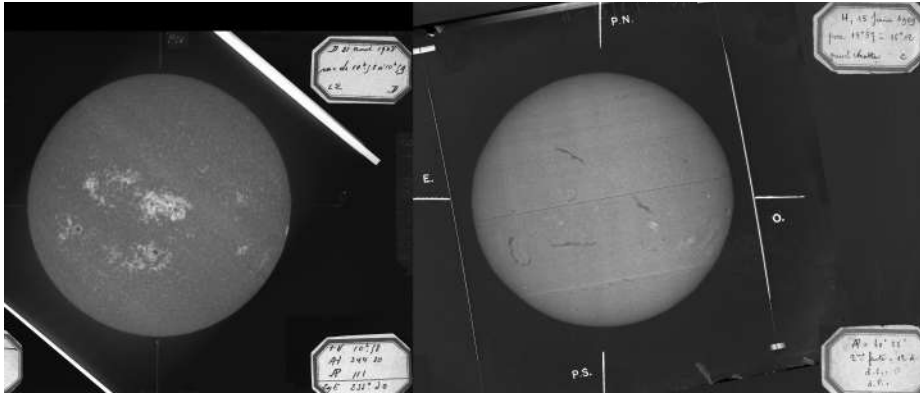


Figure 1. The Meudon collection of systematic CaII K and H α spectroheliograms started respectively in 1908 and 1909 (here images of August 31, 1908, and June 15, 1909)

- a motorized objective (geographical E/W translation) moving the solar image upon the entrance slit of the spectrograph
- dispersive elements (prisms, and later, gratings)
- a curved slit in the spectrum isolating the chosen spectral line
- a motorized photographic plate in the spectrum moving at the same speed than the imaging objective
- an artificial moon in the solar image to produce deep scans for prominences

The first **full-disk** spectroheliograms were obtained by Deslandres at Paris Observatory in 1894 using CaII K line with glass photographic plates (85.4 mm sun diameter). The first long exposure scans for prominences at the limb, using a disk attenuator, were got at the same moment. Deslandres moved from Paris to Meudon in 1898 and a new laboratory and instrument were achieved in 1906, with the collaboration of D’Azambuja (1920), who organized the solar observation routines.

Systematic observations started in 1908 for CaII K and in 1909 for H α (Figure 1). The optics and mechanics were modernized in 1985 by Olivieri. Photographic plates were abandoned in 2001. The spectroheliograph does not use a selecting slit in the spectrum anymore, and the moving plate is replaced by a fixed electronic detector. The 100 000 plates of the photographic collection are progressively digitized. Weather conditions in Meudon allow at least one daily observation between 250 and 300 days per year.

4. The new 2018 version of the spectroheliograph

As in previous versions, the solar light feeding the spectrograph (Figure 2) is caught by a coelostat (two 400 mm flat mirrors) and directed horizontally towards a 250 mm **doublet** (O1, 4000 mm focal length). It is optimized for the red (**656 nm**) and violet (**394 nm**) part of the spectrum and forms a 37.2 mm solar image on the slit of the spectrograph. **For other wavelengths, O1**

can be translated to adjust the focus. A diaphragm reduces the entrance pupil to 170 mm, providing a theoretical resolution of $1''$ in the red part of the spectrum. In practice, this resolution is reduced to $2''$ (or more) by local atmospheric turbulence.

The slit of the spectrograph has a width of 30 microns ($1.5''$ on the Sun). The entrance objective O1 is motorized, so that the solar image moves slowly in geographic E/W direction (scanning the full Sun typically takes 60 s). **This motion decreases the resolution from $1.5''$ to $2''$, but there is no consequence on image quality due to seeing conditions.**

The focal length of the collimator O2 is 1300 mm. **This doublet is unmovable and optimized for 656 and 394 nm; for other wavelengths, we insert into the beam a compensating plate.**

The dispersion device is a grating (300 groves/mm and $17^\circ 27'$ blaze angle). Incident and diffraction angles are respectively 7° and 27° . The interference order (3, 4, 5) is selected by filters behind the image plane (respectively 650, 500, 400 nm CWL and 78, 55, 66 nm FWHM). **The wavelength switching is automatic and takes 1 min.**

In the present instrument, the camera lens O3 is an **achromatic** SkyWatcher 80ED, 400 mm focal length, forming a 11.4 mm image on the detector. The new camera uses a Fairchild 2020 scientific CMOS sensor with rolling electronic shutter. It is water cooled at 5° C. This is a low noise device with 30000 dynamic range and 16 bits digitization (0.5 electron/count). The format is 2048 x 2048 square pixels (6.5 microns, 30000 electrons full well capacity). High speed readout (100 frames/s) allows fast spectroscopy. The quantum efficiency is for CaII H/K, H β and H α respectively 20%, 65% and 70%.

The spectral range is line dependant. It usually varies from 40 to 100 pixels (typically 0.5 nm to 1.0 nm, see table 1) and can be much enlarged (up to 10 nm) for specific programs upon request. The Sun is scanned using 2048 steps. The final **angular** pixel is $1.1''$ (half of the best seeing at Meudon) with 3% season fluctuation **in km.**

The exposure time is chosen to work at half saturation in far line wings (photon S/N ratio 100). It varies from 10 to 100 ms depending on line, disk attenuator, weather conditions and height of the Sun. 10 ms is typically used for H α , 20 ms for CaII H/K and 50 ms for prominences with disk attenuator (20 s to 100 s scan duration). **The speed of objective O1 is automatically adjusted to the exposure time.**

Two kinds of observations are daily performed:

- **full-disk** observations with short exposure time
- prominence observations with solar disk attenuated by an artificial moon of neutral density 0.9 (13% transmission) in the image plane (the moon avoids disk saturation of long exposure scans)

H α , H β and CaII are observed successively (but CaII H and K are simultaneous) in interference orders 3, 4 and 5. Figure 3 shows typical spectra $P_{obs}(\lambda)$ obtained near disk center. The comparison with the atlas $P_{ref}(\lambda)$ by Delbouille, Roland, and Neven (1973) recorded at the Jungfraujoeh observatory (3600 m)

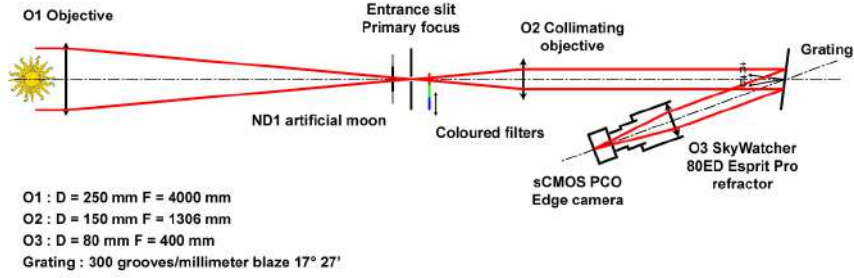


Figure 2. Optical design of the 2018 version of the spectroheliograph

Table 1. List of observable lines

Line	Wavelength (nm)	Order	Spectral Pix. (nm)	Spectral Res. (nm)	Spectral field (pixels)
H α	656.28	3	0.0155	0.025	40
H β	486.13	4	0.0116	0.019	40
CaII H	396.85	5	0.0093	0.015	100
CaII K	393.37	5	0.0093	0.015	100

with exceptional spectral resolution (0.2 pm) shows that lines are smoothed, as the spectroheliograph is designed for broad lines. A linear fit in the form $P_{obs}(\lambda) = a + b \times P_{ref}(\lambda)$ reveals in line cores a small amount of stray or parasitic light (a few %).

MP4 movies are joined as Electronic Supplemental Material to illustrate the principle of the 2018 version of the spectroheliograph (see the appendix for details). At the moment, H β is not yet operating, so that daily observations consist in one or several series of four sequences including:

- H α **full-disk** (short exposure)
- H α prominences + disk attenuator (long exposure)
- CaII H and K **full-disk** (short exposure)
- CaII H and K prominences + disk attenuator (long exposure)

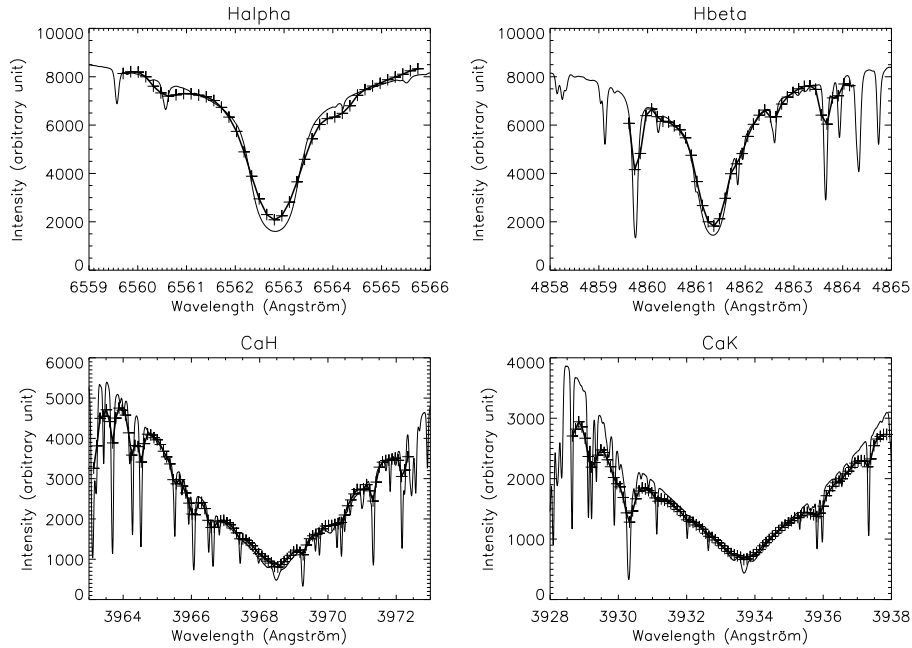


Figure 3. $H\alpha$, $H\beta$, CaII H and CaII K line profiles near disk center (thick line) in comparison with atlas profiles, from Delbouille, Roland, and Neven (1973) (thin line). Sampling points are indicated by crosses.

$H\alpha$ line profiles allow the computation of Dopplergrams, as shown by Figure 4. We used a gaussian fit to detect the wavelength position of the line, but other methods working well with similar spectral resolutions may be used, as the bisector applied by Mein (1977) to multichannel subtractive double pass observations.

5. Data levels and dissemination

We offer **to the solar community** two data levels:

- Level 0: raw data cubes, in TIFF format available via anonymous FTP and dispatched in monthly catalogues at:
<ftp://ftpbass2000.obspm.fr/pub/meudon/spc/tiff/>
- Level 1: data issued from a standard procedure and delivered by the BASS2000 solar database at:
<http://bass2000.obspm.fr/home.php?lang=en>

5.1. Level 0 data

Level 0 data are 3D raw data containing 2048 planes of spectral images (x , λ) resulting of the solar scan in y direction, except dark currents (DC) which

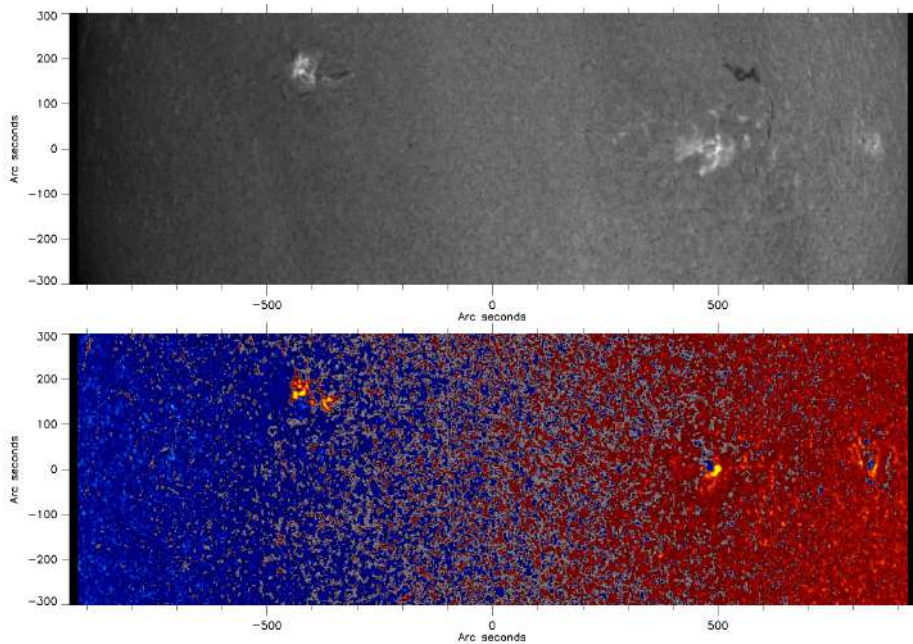


Figure 4. $H\alpha$ intensitygram and dopplergram showing solar rotation, AR12715 (left) and AR12713 (right), June 20, 2018, 08:44 UT. Intensities are not uniform because of unclear sky.

are 2D images. DC can be directly subtracted from each plane of the 3D raw observations.

More technical details and the IDL code to read raw data and reorder coordinates to produce (x, y, λ) datacubes are available here:

<https://observations-solaires.obspm.fr/Meudon-spectroheliograph-2018-version>

5.2. Level 1 data

Level 1 is the result of a standard processing applied to level 0 data, including DC subtraction, correction of the spectral line curvature (parabolic fit), rotation (P angle and coelostat position) in order to present the solar North up.

Level 1 delivers FITS 3D output containing full line profiles (x, y, λ) , classical **full-disk** images (FITS for scientific purpose and quick look JPEG) and a set with superimposition of heliographic grids or polar angle graduations.

The optical procedure to produce flat fields is complicated and under development. It will be applied in level 1 when available. Turbulence effects vary along the scan. Also, as the scanning and spectra acquisition speeds cannot be exactly equal, a residual distortion between geographic N/S and E/W may exist. It could be corrected using the method proposed by Mein and Ribes (1990).

Classical images (Figure 5) usually derived from line profiles are:

- CaII H3 and K3 line core (**full-disk** and prominences with attenuator)
- CaII H1v and K1v violet wing (-0.15 nm apart from line center)
- $H\alpha$ line core (**full-disk** and prominences with attenuator)

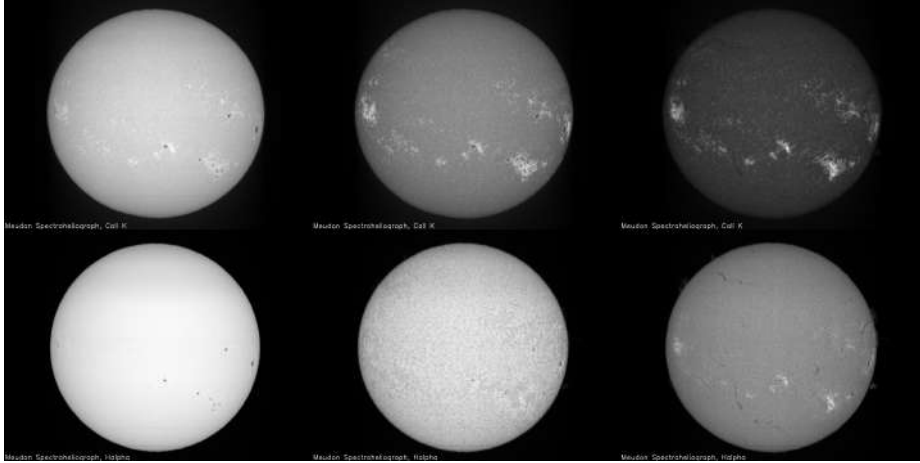


Figure 5. Example of images derived from profiles. Bottom: $H\alpha$ -0.15 nm, -0.05 nm, center. Top: CaII K -0.15 nm, -0.05 nm, center (tests of November 13, 2013)

Table 2. Spectroheliograph versions

Version	Spatial pixel (arcsec)	Spectral FOV (pixels)	Spectral pix. CaK-H α (nm)	Dynamic range (half sat.)	O3 f (mm)	output slit (μ)
PHOTO 1908-2001	1.5	1	0.015-0.025	density 3	3000	75
CCD 2002-2017	1.6	5	0.015-0.025	7500	900	
SCMOS 2018-	1.1	40-100 typical 1000 max	0.009-0.015	15000	400	

- $H\alpha$ line wings (-0.05 and +0.05 nm apart from line center)
- $H\alpha$ blue continuum (-0.15 nm apart from line center)

6. Discussion

Meudon spectroheliograph is designed for full-disk observations of broad lines as hydrogen or calcium. The characteristics of successive versions are summarized in table 2.

The photographic version (image diameter 85.4 mm, 1908-1981 on 10 x 13 cm glass plates and 1982-2001 on 13 x 18 cm film plates) is affected by defaults that are discussed by Mein and Ribes (1990). The curved slit in the spectrum (75 microns width) was removed with the first CCD (2002-2017) providing 5 wavelengths around line core. With this shutterless frame transfer CCD, a small amount of parasitic light affects differentially the 5 wavelengths during the transfer. Full line profiles are available since 2018 with a fast sCMOS sensor, which suppresses this phenomenon and has better spectral resolution and improved dynamic range. Scanning distortions still exist.

The 2018 version allows the production of monochromatic images which are more precisely centered in wavelength, with smaller bandwidth and better spatial sampling than before. Wavelength centering is now computer done, while in the former version, it was a visual inspection. Line inclination and curvature are now corrected (level 1 data only).

The availability of full line profiles is the major change since 1908. It is now possible to derive dopplergrams of active regions in $H\alpha$. The spectral range is broad (0.5 nm or more), so that large velocities can be recorded. Filament tracking, which may be affected by Dopplershifts, is improved. The spectroheliograph can follow dynamic events as flares or eruptive filaments, with moderate temporal resolution (a few minutes) in the case of full-disk scan. A faster mode is implemented for active regions (reduced FOV). However, continuous observations cannot be systematic, because of manpower limitations and meteorological conditions, but the participation to flare campaigns is possible.

Many parameters (temperature, velocity and their gradients) can be extracted from CaII line profiles. Mein *et al.* (1987) proposed a non-linear method based on Fourier series. Disturbances of Fourier coefficients were compared to theoretical disturbances of atmospheric models. Corresponding line profiles were computed using a NLTE radiative transfer code. Temperature and velocity fluctuations, together with vertical gradients, were derived from a least square inversion method. It was applied successfully to a time sequence of Ca II 396.8 nm line. Blue peaks occurring in profiles were interpreted as downward velocity gradients associated with temperature enhancement. Molowny-Horas *et al.* (1999) used another NLTE code to build a grid of $H\alpha$ lines and inverted observed profiles of filaments. Mein *et al.* (2000) made a cloud model to fit CaII 854.2 nm profiles also in the case of filaments. More recently, Beck *et al.* (2015) presented a fast inversion code for Ca II 854.2 nm. It is based on an archive of theoretical spectra that are computed under the assumption of LTE. From a comparison to NLTE inversions, they applied a first-order correction to the parameters deduced from the LTE case. Kuridze *et al.* (2017) also produced inversions of the Ca II 854.2 nm line using a NLTE code to investigate the evolution of temperature and velocity in the flaring chromosphere.

For these reasons, systematic observation of CaII infra red lines are in project for Meudon spectroheliograph.

7. Conclusion

The 2018 version of Meudon spectroheliograph is a major change since 1908. It provides full line profiles over the entire solar disk, with good spectral sampling (0.010 nm to 0.015 nm) over a 1 nm typical spectral field (up to 10 nm upon request). 3D data cubes (x, y, λ) are now **daily** produced, together with classical images at different wavelenths along the profiles. $H\alpha$, CaII H and CaII K lines are routinely observed; $H\beta$ and CaII infra red lines will come soon. Both level 0 (raw) and 1 data are available on-line **to the community**.

Spectra observed with the spectroheliograph are good indicators of solar activity in the chromosphere (active regions, faculae, filaments, prominences),

while activity in the transition region and corona is provided by SDO/AIA. The 160 and 170 nm continua observed by AIA at the top of the photosphere give images close to CaII (except filaments), so that combined ground based and space observations produce a complete diagnostic of the solar atmosphere.

The main scientific objective of Meudon spectroheliograph, with a few series of daily observations, concerns long-term solar activity, rare and extreme events, and the continuation of the 10 solar cycles collection. CaII retraces the history of the surface covered by magnetic fields, and H α memorizes chromospheric phenomena. Line profiles open new perspectives in terms of temperature and velocity determination by inversion techniques.

Data before 2002 (images in CaII K3, K1v and H α) are registered on photographic (glass or film) plates and progressively scanned. We intend to recover the production of synoptic maps using automated procedures (Aboudarham *et al.*, 2008).

A complementary short-term and automatic survey at high temporal resolution (20 s) for observations of transient activity (fares, filament eruption, CME onset, Moreton waves) is under development for Calern Observatory using monochromatic H α and CaII K filters; this will be the topic of a next paper.

*If you use data for publication, please insert the following acknowledgment :
"Meudon spectroheliograph data are courtesy of the solar and BASS2000 teams,
as part of operational services of Paris Observatory"*

Acknowledgments This paper is dedicated to the memory of Dr E. Ribes who directed Meudon solar observations during many years and passed prematurely away in 1996.

We thank the referee for helpful comments and suggestions. We are also indebted to the technical staff of LESIA (D. Crussaire, N. Füller, C. Imad, M. Ortiz, C. Renié and D. Ziegler) and to the team of observers which operate daily the instrument (C. Blanchard, I. Bualé, S. Cnudde, A. Docclo, I. Ibntaieb). We are grateful to the Scientific Council of Paris Observatory for financial support and INSU/CNRS for the label of National Observing Service (SNO). K.D. is supported by the Centre National d'Etudes Spatiales (CNES).

Appendix

Electronic Supplemental Material (movies in MPEG 4 format).

- Movie 1: the principle of the 2018 version of Meudon spectroheliograph in the case of CaII K line. The surface of the sun (right) is scanned by a thin slit and full line profiles (left) are registered for the 2048 positions of the slit. Data are stored in 3D files (2 space coordinates + spectral line). The scan time takes about 60 s using a 1.5'' slit.
- Movie 2: same as movie 1, but for H α line.
- Movie 3: example of images got at different wavelength positions along the line profiles. Part 1: H α ; part 2: CaII K.

References

- Aboudarham, J., Scholl, I., Fuller, N., Fouesneau, M., Galametz, M., Gonon, F., Maire, A., Leroy, Y.: 2008, Automatic detection and tracking of filaments for a solar feature database. *Annales Geophysicae* **26**, 243. DOI. ADS.
- Aulanier, G., Démoulin, P., Schrijver, C.J., Janvier, M., Pariat, E., Schmieder, B.: 2013, The standard flare model in three dimensions. II. Upper limit on solar flare energy. *Astron. Astrophys.* **549**, A66. DOI. ADS.
- Beck, C., Choudhary, D.P., Rezaei, R., Louis, R.E.: 2015, Fast Inversion of Solar Ca II Spectra. *Astrophys. J.* **798**, 100. DOI. ADS.
- Bertello, L., Ulrich, R.K., Boyden, J.E.: 2010, The Mount Wilson Ca ii K Plage Index Time Series. *Solar Phys.* **264**, 31. DOI. ADS.
- Carrington, R.C.: 1859, Description of a Singular Appearance seen in the Sun on September 1, 1859. *Mon. Not. Roy. Astron. Soc.* **20**, 13. DOI. ADS.
- Charbonneau, P.: 2010, Dynamo Models of the Solar Cycle. *Living Reviews in Solar Physics* **7**, 3. DOI. ADS.
- Chatzistergos, T., Ermolli, I., Solanki, S.K., Krivova, N.A.: 2018, Analysis of full disc Ca II K spectroheliograms. I. Photometric calibration and centre-to-limb variation compensation. *Astron. Astrophys.* **609**, A92. DOI. ADS.
- Crosby, N.B., Aschwanden, M.J., Dennis, B.R.: 1993, Frequency distributions and correlations of solar X-ray flare parameters. *Solar Phys.* **143**, 275. DOI. ADS.
- D'Azambuja, L.: 1920, Le Spectrohéliographe. *L'Astronomie* **34**, 487. ADS.
- Delbouille, L., Roland, G., Neven, L.: 1973, *Atlas photométrique du spectre solaire de $[\lambda] 3000$ à $[\lambda] 10000$* . ADS.
- Deslandres, H.: 1909, On the progressive revelation of the entire atmosphere of the Sun. *The Observatory* **32**, 282. ADS.
- Ellison, M.A.: 1946, Visual and spectrographic observations of a great solar flare, 1946 July 25. *Mon. Not. Roy. Astron. Soc.* **106**, 500. DOI. ADS.
- Fontenla, J.M., Harder, J., Livingston, W., Snow, M., Woods, T.: 2011, High-resolution solar spectral irradiance from extreme ultraviolet to far infrared. *Journal of Geophysical Research (Atmospheres)* **116**, D20108. DOI. ADS.
- Gallagher, P.T., Denker, C., Yurchyshyn, V., Spirock, T., Qiu, J., Wang, H., Goode, P.R.: 2002, Solar activity monitoring and forecasting capabilities at Big Bear Solar Observatory. *Annales Geophysicae* **20**, 1105. DOI. ADS.
- Garcia, A., Sobotka, M., Klvaňa, M., Bumba, V.: 2011, Synoptic observations with the Coimbra spectroheliograph. *Contributions of the Astronomical Observatory Skalnaté Pleso* **41**, 69. ADS.
- Hagh, J.D.: 2007, The Sun and the Earth's Climate. *Living Reviews in Solar Physics* **4**, 2. DOI. ADS.
- Hale, G.E.: 1907, Some New Applications of the Spectroheliograph. *Astrophys. J.* **25**, 311. DOI. ADS.
- Hale, G.E., Ellerman, F., Nicholson, S.B., Joy, A.H.: 1919, The Magnetic Polarity of Sun-Spots. *Astrophys. J.* **49**, 153. DOI. ADS.
- Harvey, J.W., Bolding, J., Clark, R., Hauth, D., Hill, F., Kroll, R., Luis, G., Mills, N., Purdy, T., Henney, C., Holland, D., Winter, J.: 2011, Full-disk Solar H-alpha Images From GONG. In: *AAS/Solar Physics Division Abstracts #42, Bulletin of the American Astronomical Society* **43**, 17.45. ADS.
- Hasan, S.S., Mallik, D.C.V., Bagare, S.P., Rajaguru, S.P.: 2010, Solar Physics at the Kodaikanal Observatory: A Historical Perspective. *Astrophysics and Space Science Proceedings* **19**, 12. DOI. ADS.
- Hathaway, D.H.: 2010, The Solar Cycle. *Living Reviews in Solar Physics* **7**, 1. DOI. ADS.
- Hathaway, D.H., Wilson, R.M., Reichmann, E.J.: 2002, Group Sunspot Numbers: Sunspot Cycle Characteristics. *Solar Phys.* **211**, 357. DOI. ADS.
- Hodgson, R.: 1859, On a curious Appearance seen in the Sun. *Mon. Not. Roy. Astron. Soc.* **20**, 15. DOI. ADS.
- Hoyt, D.V., Schatten, K.H.: 1998, Group Sunspot Numbers: A New Solar Activity Reconstruction. *Solar Phys.* **181**, 491. DOI. ADS.
- Karna, N., Pesnell, W.D., Zhang, J.: 2015, A comprehensive study of cavities on the Sun: Structures and Evolution. In: *AGU Fall Meeting Abstracts* **2015**, SH54B. ADS.
- Krucker, S., Benz, A.O.: 1998, Energy Distribution of Heating Processes in the Quiet Solar Corona. *Astrophys. J.* **501**, L213. DOI. ADS.

- Kuridze, D., Henriques, V., Mathioudakis, M., Koza, J., Zaqarashvili, T.V., Rybák, J., Hanslmeier, A., Keenan, F.P.: 2017, Spectroscopic Inversions of the Ca II 8542 Å Line in a C-class Solar Flare. *Astrophys. J.* **846**, 9. DOI. ADS.
- Lean, J.L.: 2018, Estimating Solar Irradiance Since 850 CE. *Earth and Space Science* **5**, 133. DOI. ADS.
- Leroy, J.L., Bommier, V., Sahal-Brechot, S.: 1983, The magnetic field in the prominences of the polar crown. *Solar Phys.* **83**, 135. DOI. ADS.
- Makarov, V.I., Sivaraman, K.R.: 1989, New Results Concerning the Global Solar-Cycle. *Solar Phys.* **123**, 367. DOI. ADS.
- Martres, M.-J., Zlicaric, G.: 1982, L'activité solaire, cartes synoptiques de la chromosphère et des taches. *L'Astronomie* **96**, 45. ADS.
- Mein, P.: 1977, Multi-channel subtractive spectrograph and filament observations. *Solar Phys.* **54**, 45. DOI. ADS.
- Mein, P., Ribes, E.: 1990, Spectroheliograms and motions of magnetic tracers. *Astron. Astrophys.* **227**, 577. ADS.
- Mein, P., Mein, N., Malherbe, J.M., Dame, L.: 1987, Inversion of line profile disturbances - A nonlinear method applied to solar CaII lines. *Astron. Astrophys.* **177**, 283. ADS.
- Mein, P., Briand, C., Heinzel, P., Mein, N.: 2000, Solar arch filaments observed with THEMIS. *Astron. Astrophys.* **355**, 1146. ADS.
- Molowny-Horas, R., Heinzel, P., Mein, P., Mein, N.: 1999, A non-LTE inversion procedure for chromospheric cloud-like features. *Astron. Astrophys.* **345**, 618. ADS.
- Mouradian, Z., Soru-Escout, I.: 1993, On solar activity and the solar cycle. A new analysis of the Butterfly Diagram of sunspots. *Astron. Astrophys.* **280**, 661. ADS.
- Mouradian, Z., Soru-Escout, I.: 1994, A new analysis of the butterfly diagram for solar filaments. *Astron. Astrophys.* **290**, 279. ADS.
- Norton, A.A., Charbonneau, P., Passos, D.: 2014, Hemispheric Coupling: Comparing Dynamo Simulations and Observations. *Space Sci. Rev.* **186**, 251. DOI. ADS.
- Parnell, C.E., Jupp, P.E.: 2000, Statistical Analysis of the Energy Distribution of Nanoflares in the Quiet Sun. *Astrophys. J.* **529**, 554. DOI. ADS.
- Petrovay, K.: 2010, Solar Cycle Prediction. *Living Reviews in Solar Physics* **7**, 6. DOI. ADS.
- Pevtsov, A.A., Virtanen, I., Mursula, K., Tlatov, A., Bertello, L.: 2016, Reconstructing solar magnetic fields from historical observations. I. Renormalized Ca K spectroheliograms and pseudo-magnetograms. *Astron. Astrophys.* **585**, A40. DOI. ADS.
- Ribes, E., Bonfond, F.: 1990, Magnetic tracers, a probe of the solar convective layers. *Geophysical and Astrophysical Fluid Dynamics* **55**, 241. DOI. ADS.
- Schmieder, B.: 2018, Extreme solar storms based on solar magnetic field. *Journal of Atmospheric and Solar-Terrestrial Physics* **180**, 46. DOI. ADS.
- Schrijver, C.J., Beer, J., Baltensperger, U., Cliver, E.W., Güdel, M., Hudson, H.S., McCracken, K.G., Osten, R.A., Peter, T., Soderblom, D.R., Usoskin, I.G., Wolff, E.W.: 2012, Estimating the frequency of extremely energetic solar events, based on solar, stellar, lunar, and terrestrial records. *Journal of Geophysical Research (Space Physics)* **117**, A08103. DOI. ADS.
- Schwabe, H.: 1844, Sonnenbeobachtungen im Jahre 1843. Von Herrn Hofrath Schwabe in Dessau. *Astronomische Nachrichten* **21**, 233. DOI. ADS.
- Secchi, A.: 1875, *Le Soleil*. DOI. ADS.
- Shimizu, T., Tsuneta, S.: 1997, Deep Survey of Solar Nanoflares with Yohkoh. *Astrophys. J.* **486**, 1045. DOI. ADS.
- Tobias, S.M.: 2002, The solar dynamo. *Philosophical Transactions of the Royal Society of London Series A* **360**, 2741. DOI. ADS.
- Toriumi, S., Schrijver, C.J., Harra, L.K., Hudson, H., Nagashima, K.: 2017, Magnetic Properties of Solar Active Regions That Govern Large Solar Flares and Eruptions. *Astrophys. J.* **834**, 56. DOI. ADS.
- Wolf, R.: 1861, Abstract of his latest Results. *Mon. Not. Roy. Astron. Soc.* **21**, 77. DOI. ADS.